σ exchange in the one-boson exchange model involving the ground state octet baryons

Bing Wu,[1,2,*] Xiong-Hui Cao,[1,†] Xiang-Kun Dong,[3,‡] and Feng-Kun Guo[1,2,4,5,§]

[1]*CAS Key Laboratory of Theoretical Physics, Institute of Theoretical Physics, Chinese Academy of Sciences, Beijing 100190, China*
[2]*School of Physical Sciences, University of Chinese Academy of Sciences, Beijing 100049, China*
[3]*Helmholtz-Institut für Strahlen- und Kernphysik and Bethe Center for Theoretical Physics, Universität Bonn, D-53115 Bonn, Germany*
[4]*Peng Huanwu Collaborative Center for Research and Education, Beihang University, Beijing 100191, China*
[5]*Southern Center for Nuclear-Science Theory, Institute of Modern Physics, Huizhou 516000, China*

(Received 8 December 2023; accepted 25 January 2024; published 26 February 2024)

Based on the one-boson-exchange framework that the σ meson serves as an effective parametrization for the correlated scalar-isoscalar $\pi\pi$ interaction, we calculate the coupling constants of the σ to the $\frac{1}{2}^+$ ground state light baryon octet $\mathbb{B}$ by matching the amplitude of $\mathbb{B}\bar{\mathbb{B}} \to \pi\pi \to \bar{\mathbb{B}}\mathbb{B}$ to that of $\mathbb{B}\bar{\mathbb{B}} \to \sigma \to \bar{\mathbb{B}}\mathbb{B}$. The former is calculated using a dispersion relation, supplemented with chiral perturbation theory results for the $\mathbb{B}\mathbb{B}\pi\pi$ couplings and the Muskhelishvili-Omnès representation for the $\pi\pi$ rescattering. Explicitly, the coupling constants are obtained as $g_{NN\sigma} = 8.7^{+1.7}_{-1.9}$, $g_{\Sigma\Sigma\sigma} = 3.5^{+1.8}_{-1.3}$, $g_{\Xi\Xi\sigma} = 2.5^{+1.5}_{-1.4}$, and $g_{\Lambda\Lambda\sigma} = 6.8^{+1.5}_{-1.7}$. These coupling constants can be used in the one-boson-exchange model calculations of the interaction of light baryons with other hadrons.

DOI: 10.1103/PhysRevD.109.034026

I. INTRODUCTION

In the past few decades, the observation of exotic hadronic states, which cannot be accounted for by the conventional quark model, has propelled the study of exotic states to the forefront of hadron physics; see Refs. [1–14] for recent reviews on the experimental and theoretical status. Hadronic molecules [7], one of the most promising candidates for exotic states, are loosely bound states of hadrons and a natural extension of the atomic nuclei (such as the deuteron as a proton-neutron bound state) and offer an explanation of the many experimentally observed near-threshold structures, in particular in the heavy-flavor hadron mass region [15].

As a generalization of the one-pion-exchange potential [16], the one-boson-exchange (OBE) model has played a crucial role in studying composite systems of hadrons [10,11,17–25]. Taking the deuteron as an example, it is widely accepted in the OBE model that its formation involves the long-range interaction from the one-pion exchange and the middle-range interaction from the σ-meson exchange; see Ref. [18] for a detailed review. However, unlike narrow width particles that are associated with clear resonance peaks or dips observed in experiments, the scalar-isoscalar σ meson, which plays a crucial role in nuclear and hadron physics, had remained a subject of considerable debates for several decades until it was established as the lowest-lying hadronic resonance in quantum chromodynamics (QCD) in the past 20 years based on rigorous dispersive analyses of $\pi\pi$ scattering [26–28] (see, e.g., Refs. [29,30] for reviews). The dispersive techniques have recently been applied to determine the nature of the σ at unphysical pion masses [31,32].

The σ meson in the OBE model can be considered as approximating the correlated S-wave isoscalar $\pi\pi$ exchange in a few hundred MeV range [18,33–38], and some modifications to its properties have been made in order to improve the accuracy of the approximation [18,33]. However, the effective coupling constants between the σ and various hadrons remain highly uncertain. One example is the widely used nucleon-nucleon-σ coupling $g_{NN\sigma}$, which ranges roughly from 8 to 14 [18,33,36]. For its couplings to other ground state octet baryons, $g_{\Sigma\Sigma\sigma}$, $g_{\Xi\Xi\sigma}$, and $g_{\Lambda\Lambda\sigma}$, there are rare systematic discussions and error analyses. Most of

*wubing@itp.ac.cn
†xhcao@itp.ac.cn
‡xiangkun@hiskp.uni-bonn.de
§fkguo@itp.ac.cn

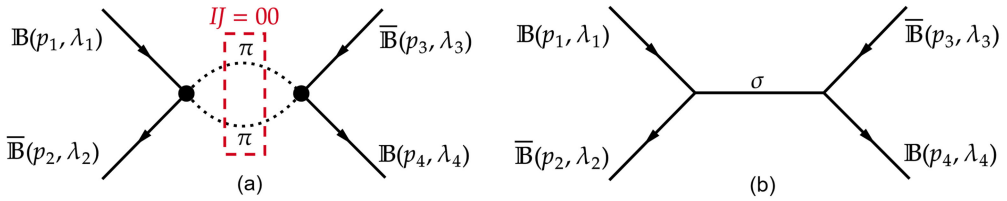

FIG. 1. Feynman diagrams for the s-channel process of $\mathbb{B}\bar{\mathbb{B}} \to \bar{\mathbb{B}}\mathbb{B}$ with the intermediate state of $\pi\pi$ (a) or σ (b). In (a), the black dots imply that the $\pi\pi$ rescattering is included.

them are estimated either by the quenched quark model or the SU(3) symmetry model assuming the σ to be a certain member of the light-flavor multiplet [23,24]. The use of the one-σ exchange instead of the correlated $\pi\pi$ exchange may raise some questions: Is this approximation reasonable? How good is the approximation? In the present work, we try to address these questions by considering the scattering of the baryon and antibaryon in the ground state octet, $\mathbb{B}\bar{\mathbb{B}} \to \bar{\mathbb{B}}\mathbb{B}$, through the intermediate state of the correlated $IJ = 00$ $\pi\pi$ pair or the σ meson and calculate the effective coupling constants of $g_{\mathbb{B}\mathbb{B}\sigma}$. We will make use of dispersion relations following Ref. [39], and similar methods have been used in, e.g., Refs. [37,38] to derive the baryon-baryon-σ couplings, and Ref. [40] to derive the σ coupling to heavy mesons. Here, we will match the dispersive amplitudes of $\mathbb{B}\bar{\mathbb{B}} \to \pi\pi$ at low energies to the chiral amplitudes up to the next-to-leading order (NLO).

This paper is structured as follows. The formalism is presented in Sec. II, including the calculation of the OBE amplitude in Sec. II A and the amplitude from the dispersion relation (DR) with a careful treatment of kinematical singularities in Sec. II B. In Sec. III, we conduct an analysis of the two amplitudes and present the scalar coupling constants $g_{\mathbb{B}\mathbb{B}\sigma}$ along with an error analysis. This includes a comparison of the s-channel processes, as detailed in Sec. III A, and a comparison of the corresponding t/u-channel processes utilizing the crossing symmetry in Sec. III B. A brief summary is given in Sec. IV. The adopted conventions, the result of $NN\sigma$ coupling in the SU(2) framework, and crossing symmetry relations are relegated to the Appendixes.

II. FORMALISM

To determine the scalar coupling, $g_{\mathbb{B}\mathbb{B}\sigma}$, between the baryon $\mathbb{B}$ in the $\frac{1}{2}^+$ ground baryon octet and the σ meson, we first utilize the DR and chiral perturbation theory (ChPT) to calculate the amplitude of $\mathbb{B}(p_1,\lambda_1) + \bar{\mathbb{B}}(p_2,\lambda_2) \to \bar{\mathbb{B}}(p_3,\lambda_3) + \mathbb{B}(p_4,\lambda_4)$ with a correlated $\pi\pi$ intermediate state, as depicted in Fig. 1(a). Here, p_i and λ_i represent the four momentum and the helicity of particle $\mathbb{B}$ or $\bar{\mathbb{B}}$, respectively. Additionally, we restrict the quantum numbers of the two-body intermediate state, $\pi\pi$, to be $IJ = 00$. This S-wave amplitude can be denoted as $\mathcal{M}^{\rm DR}_{\mathbb{B}(\lambda_1)+\bar{\mathbb{B}}(\lambda_2)\to\bar{\mathbb{B}}(\lambda_3)+\mathbb{B}(\lambda_4),0}(s)$, where the subscript 0 indicates the S-wave, s represents the square of the total energy of the system in the c.m. frame,[1] and the superscript DR indicates the result obtained from the DR. Next, we proceed to calculate the same amplitude, with the intermediate σ meson, as depicted in Fig. 1(b). In this case, we utilize the OBE model, and the corresponding amplitude can be expressed as $\mathcal{M}^{\rm OBE}_{\mathbb{B}(\lambda_1)+\bar{\mathbb{B}}(\lambda_2)\to\bar{\mathbb{B}}(\lambda_3)+\mathbb{B}(\lambda_4)}(s)$. Finally, we compare the aforementioned amplitudes to extract the coupling constant $g_{\mathbb{B}\mathbb{B}\sigma}$ in the phenomenological baryon-baryon-σ coupling Lagrangian.

A. The OBE amplitude

According to the following effective Lagrangian coupling the σ meson to the baryons in the SU(3) flavor octet [18,41],

$$\begin{aligned}
\mathcal{L}_{\Sigma\Sigma\sigma} &= -g_{\Sigma\Sigma\sigma}(\bar{\Sigma}^+\Sigma^- + \bar{\Sigma}^0\Sigma^0 + \bar{\Sigma}^-\Sigma^+)\sigma,\\
\mathcal{L}_{\Xi\Xi\sigma} &= -g_{\Xi\Xi\sigma}(\bar{\Xi}^0\Xi^0 + \bar{\Xi}^+\Xi^-)\sigma,\\
\mathcal{L}_{\Lambda\Lambda\sigma} &= -g_{\Lambda\Lambda\sigma}\bar{\Lambda}\Lambda\sigma,\\
\mathcal{L}_{NN\sigma} &= -g_{NN\sigma}(\bar{p}p + \bar{n}n)\sigma,
\end{aligned} \tag{1}$$

the OBE amplitude for the Feynman diagram depicted in Fig. 1(b) reads

$$\begin{aligned}
&\mathcal{M}^{\rm OBE}_{\mathbb{B}(\lambda_1)+\bar{\mathbb{B}}(\lambda_2)\to\bar{\mathbb{B}}(\lambda_3)+\mathbb{B}(\lambda_4)}\\
&\quad = C_{\mathbb{B}} g^2_{\mathbb{B}\mathbb{B}\sigma} \frac{\bar{v}^{\lambda_2}(p_2)u^{\lambda_1}(p_1)\bar{u}^{\lambda_4}(p_4)v^{\lambda_3}(p_3)}{(p_1+p_2)^2 - m_\sigma^2},
\end{aligned} \tag{2}$$

where $C_{\mathbb{B}}$ is a flavor factor, $C_\Sigma = 3$, $C_\Xi = -2$, $C_\Lambda = 1$, and $C_N = -2$. For simplicity, we choose $\lambda_i = 1/2$ $(i = 1,\ldots,4)$ throughout the paper.[2] With this choice we have

$$\mathcal{M}^{\rm OBE}_{\mathbb{B}\bar{\mathbb{B}}\to\bar{\mathbb{B}}\mathbb{B}}(s) = C_{\mathbb{B}} g^2_{\mathbb{B}\mathbb{B}\sigma} \frac{s - 4m^2_{\mathbb{B}}}{s - m_\sigma^2}, \tag{3}$$

where $m_{\mathbb{B}}$ is the isospin averaged mass of the baryon $\mathbb{B}$.[3]

[1] For an s-channel process of $\mathbb{B}(p_1)+\bar{\mathbb{B}}(p_2)\to\bar{\mathbb{B}}(p_3)+\mathbb{B}(p_4)$, as illustrated in Fig. 1, $s = (p_1+p_2)^2$ while $t = (p_1-p_3)^2$.

[2] Other choices, e.g., physical amplitudes using the orbital-spin basis are also accessible. The final results do not depend on the choice.

[3] Since we are not interested in the isospin symmetry breaking effects, the isospin averaged mass is used for all particles within the same isospin multiplet.

B. The dispersive representation

1. The DR and the kinematical singularity

One can write down a dispersive representation of the $\mathbb{B}\bar{\mathbb{B}}$ scattering amplitude corresponding to Fig. 1(a) as

$$\mathcal{M}^{\rm DR}_{\mathbb{B}\bar{\mathbb{B}}\to\bar{\mathbb{B}}\mathbb{B},0}(s)=\frac{s-4m_{\mathbb{B}}^2}{2\pi i}\int_{4M_\pi^2}^{+\infty}\frac{{\rm disc}[\mathcal{M}^{\rm DR}_{\mathbb{B}\bar{\mathbb{B}}\to\bar{\mathbb{B}}\mathbb{B},0}(z)]}{(z-s)(z-4m_{\mathbb{B}}^2)}{\rm d}z. \quad (4)$$

Here a once-subtracted dispersive integral is employed to facilitate the convergence of the dispersive integral. The threshold $s=4m_{\mathbb{B}}^2$ is chosen as the subtraction point, and we set the subtraction constant $\mathcal{M}^{\rm DR}(s=4m_{\mathbb{B}}^2)=0$ as Eq. (3) since the two amplitudes will be matched later.

In order to capture the $\pi\pi$ rescattering in the σ region and avoid the interference from other resonances, e.g., the $f_0(980)$, the upper limit of the dispersive integral in Eq. (4) is set to $s_0=(0.8\ {\rm GeV})^2$, as in Ref. [39] (see also Ref. [42]). We will investigate the impact of varying the upper limit of the integration on the final result and regard it as a part of the uncertainty of the coupling constants.

Next, let us discuss the discontinuity. Taking into account the unitary relation that is fulfilled by the partial-wave T-matrix elements, we can express the discontinuity of the S-wave amplitude (here the partial wave refers to that between the pions) along the cut $s\in[4M_\pi^2,+\infty)$ in terms of $T_{\mathbb{B}\bar{\mathbb{B}}\to\pi\pi,0}(s)$ and $T_{\pi\pi\to\bar{\mathbb{B}}\mathbb{B},0}(s)$. However, it is crucial to notice that when dealing with systems that involve spins, particularly those containing fermions, kinematical singularities arise [43]. These singularities stem from the definition of the wave functions for the initial and final states. Following Ref. [43], we introduce the kinematical-singularity-free amplitudes,

$$T^{\rm new}_{\mathbb{B}\bar{\mathbb{B}}\to\pi\pi,0}(s)=\sqrt{s-4m_{\mathbb{B}}^2}\,T_{\mathbb{B}\bar{\mathbb{B}}\to\pi\pi,0}(s), \quad (5)$$

$$T^{\rm new}_{\pi\pi\to\bar{\mathbb{B}}\mathbb{B},0}(s)=\sqrt{s-4m_{\mathbb{B}}^2}\,T_{\pi\pi\to\bar{\mathbb{B}}\mathbb{B},0}(s). \quad (6)$$

Then the unitary relation for the S-wave T-matrix elements is given by

$${\rm disc}[\mathcal{M}_{\mathbb{B}\bar{\mathbb{B}}\to\bar{\mathbb{B}}\mathbb{B},0}(s)]=2i\rho_\pi(s)\frac{T^{\rm new}_{\mathbb{B}\bar{\mathbb{B}}\to\pi\pi,0}(s)T^{\rm new*}_{\pi\pi\to\bar{\mathbb{B}}\mathbb{B},0}(s)}{s-4m_{\mathbb{B}}^2}\times\theta(\sqrt{s}-2M_\pi), \quad (7)$$

where $\rho_\pi(s)=\frac{1}{16\pi}\sqrt{\frac{s-4M_\pi^2}{s}}$ is the two-body phase space factor. Moreover, as we will discuss in detail in Sec. II B 4, the treatment of kinematical singularity plays a vital role in guaranteeing the self-consistency of the theory.

Furthermore, with the phase conventions outlined in Appendix A and considering the isospin scalar $\pi\pi$ system, we obtain the following relations:

$$\begin{aligned}
T_{\Sigma\bar{\Sigma}\to\pi\pi,0}(s)&=-T_{\pi\pi\to\bar{\Sigma}\Sigma,0}(s),\\
T_{\Xi\bar{\Xi}\to\pi\pi,0}(s)&=T_{\pi\pi\to\bar{\Xi}\Xi,0}(s),\\
T_{\Lambda\bar{\Lambda}\to\pi\pi,0}(s)&=-T_{\pi\pi\to\bar{\Lambda}\Lambda,0}(s),\\
T_{N\bar{N}\to\pi\pi,0}(s)&=T_{\pi\pi\to\bar{N}N,0}(s).
\end{aligned} \quad (8)$$

Then, we obtain the following discontinuities,

$${\rm disc}[\mathcal{M}_{\Sigma\bar{\Sigma}\to\bar{\Sigma}\Sigma,0}(s)]=2i\rho_\pi\frac{-|T^{\rm new}_{\Sigma\bar{\Sigma}\to\pi\pi,0}(s)|^2}{s-4m_\Sigma^2}\theta(\sqrt{s}-2M_\pi), \quad (9)$$

$${\rm disc}[\mathcal{M}_{\Xi\bar{\Xi}\to\bar{\Xi}\Xi,0}(s)]=2i\rho_\pi\frac{|T^{\rm new}_{\Xi\bar{\Xi}\to\pi\pi,0}(s)|^2}{s-4m_\Xi^2}\theta(\sqrt{s}-2M_\pi), \quad (10)$$

$${\rm disc}[\mathcal{M}_{\Lambda\bar{\Lambda}\to\bar{\Lambda}\Lambda,0}(s)]=2i\rho_\pi\frac{-|T^{\rm new}_{\Lambda\bar{\Lambda}\to\pi\pi,0}(s)|^2}{s-4m_\Lambda^2}\theta(\sqrt{s}-2M_\pi), \quad (11)$$

$${\rm disc}[\mathcal{M}_{N\bar{N}\to\bar{N}N,0}(s)]=2i\rho_\pi\frac{|T^{\rm new}_{N\bar{N}\to\pi\pi,0}(s)|^2}{s-4m_N^2}\theta(\sqrt{s}-2M_\pi). \quad (12)$$

2. The SU(3) ChPT framework

To obtain the low-energy S-wave amplitudes $T_{\mathbb{B}\bar{\mathbb{B}}\to\pi\pi,0}(s)$, we need the corresponding chiral baryon-meson Lagrangian. The leading-order (LO) chiral Lagrangian is given by [44]

$$\begin{aligned}
\mathcal{L}^{(1)}_{\mathbb{M}\mathbb{B}}&=\langle\bar{\mathbb{B}}(i\mathcal{D}-m_0)\mathbb{B}\rangle+\frac{D}{2}\langle\bar{\mathbb{B}}\gamma^\mu\gamma_5\{u_\mu,\mathbb{B}\}\rangle\\
&\quad+\frac{F}{2}\langle\bar{\mathbb{B}}\gamma^\mu\gamma_5[u_\mu,\mathbb{B}]\rangle,
\end{aligned} \quad (13)$$

which contains three low-energy constants (LECs), m_0, D, and F. Here, $\langle\cdot\rangle$ means trace in the flavor space, the baryon octet are collected in the matrix,

$$\mathbb{B}=\begin{pmatrix}\frac{1}{\sqrt{2}}\Sigma^0+\frac{1}{\sqrt{6}}\Lambda & \Sigma^+ & p\\ \Sigma^- & -\frac{1}{\sqrt{2}}\Sigma^0+\frac{1}{\sqrt{6}}\Lambda & n\\ \Xi^- & \Xi^0 & -\frac{2}{\sqrt{6}}\Lambda\end{pmatrix}, \quad (14)$$

and the chiral vielbein and covariant derivative are given by

$$\begin{aligned}
&u_\mu=iu^\dagger\partial_\mu u-iu\partial_\mu u^\dagger,\qquad \mathcal{D}_\mu\mathbb{B}=\partial_\mu B+[\Gamma_\mu,B],\\
&\Gamma_\mu=\frac{1}{2}(u^\dagger\partial_\mu u+u\partial_\mu u^\dagger),
\end{aligned} \quad (15)$$

with $u^2=U$, $U=\exp(i\sqrt{2}\Phi/F_\pi)$, where

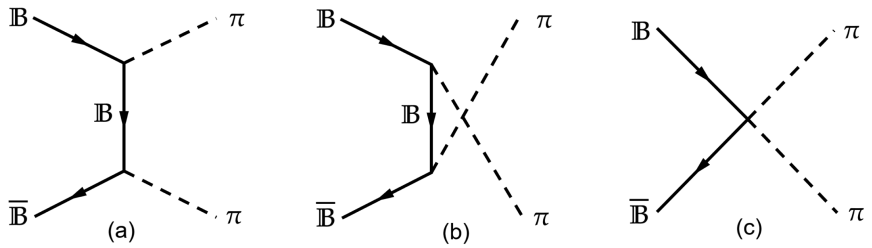

FIG. 2. The tree-level Feynman diagrams for the process of $\mathbb{B}\bar{\mathbb{B}} \to \pi\pi$.

$$\Phi = \begin{pmatrix} \frac{\pi^0}{\sqrt{2}} + \frac{\eta}{\sqrt{6}} & \pi^+ & K^+ \\ \pi^- & -\frac{\pi^0}{\sqrt{2}} + \frac{\eta}{\sqrt{6}} & K^0 \\ K^- & \bar{K}^0 & -\frac{2}{\sqrt{6}}\eta \end{pmatrix}. \tag{16}$$

Notice that the chiral connection Γ_μ containing two pions is a vector, the two pions from that term cannot be in the S wave. As a result, only the t- and u-channel exchanges depicted in Figs. 2(a) and 2(b), which contribute to the LHC part of $T_{\mathbb{B}\bar{\mathbb{B}}\to\pi\pi,0}(s)$, will be present in the LO calculation. In addition, the LO Lagrangian contains the $\Sigma\Lambda\pi$ coupling terms of the form $\bar{\Lambda}\gamma^\mu\gamma_5\partial_\mu\pi\Sigma$ and $\bar{\Sigma}\gamma^\mu\gamma_5\partial_\mu\pi\Lambda$. Therefore, it is necessary to consider the exchange of Σ in the $\Lambda\bar{\Lambda} \to \pi\pi$ process and the exchange of Λ in the $\Sigma\bar{\Sigma} \to \pi\pi$ process.

The $\mathcal{O}(p^2)$ chiral Lagrangian contains the $\bar{\mathbb{B}}\mathbb{B}\pi\pi$ contact contribution with the S-wave pion pair, as illustrated in Fig. 2(c). At the NLO, the number of LECs increases, and the Lagrangian reads [45,46][4]

$$\begin{aligned}\mathcal{L}^{(2)}_{\mathbb{MB}} = {} & b_D\langle\bar{\mathbb{B}}\{\chi_+,\mathbb{B}\}\rangle + b_F\langle\bar{\mathbb{B}}[\chi_+,\mathbb{B}]\rangle + b_0\langle\bar{\mathbb{B}}\mathbb{B}\rangle\langle\chi_+\rangle + b_1\langle\bar{\mathbb{B}}[u^\mu,[u_\mu,\mathbb{B}]]\rangle + b_2\langle\bar{\mathbb{B}}\{u^\mu,\{u_\mu,\mathbb{B}\}\}\rangle \\ & + b_3\langle\bar{\mathbb{B}}\{u^\mu,[u_\mu,\mathbb{B}]\}\rangle + b_4\langle\bar{\mathbb{B}}\mathbb{B}\rangle\langle u^\mu u_\mu\rangle + ib_5(\langle\bar{\mathbb{B}}[u^\mu,[u^\nu,\gamma_\mu\mathcal{D}_\nu\mathbb{B}]]\rangle - \langle\bar{\mathbb{B}}\overleftarrow{\mathcal{D}}_\nu[u^\nu,[u^\mu,\gamma_\mu\mathbb{B}]]\rangle) \\ & + ib_6(\langle\bar{\mathbb{B}}[u^\mu,\{u^\nu,\gamma_\mu\mathcal{D}_\nu\mathbb{B}\}]\rangle - \langle\bar{\mathbb{B}}\overleftarrow{\mathcal{D}}_\nu\{u^\nu,[u^\mu,\gamma_\mu\mathbb{B}]\}\rangle) + ib_7(\langle\bar{\mathbb{B}}\{u^\mu,\{u^\nu,\gamma_\mu\mathcal{D}_\nu\mathbb{B}\}\}\rangle - \langle\bar{\mathbb{B}}\overleftarrow{\mathcal{D}}_\nu\{u^\nu,\{u^\mu,\gamma_\mu\mathbb{B}\}\}\rangle) \\ & + ib_8(\langle\bar{\mathbb{B}}\gamma_\mu\mathcal{D}_\nu\mathbb{B}\rangle - \langle\bar{\mathbb{B}}\overleftarrow{\mathcal{D}}_\nu\gamma_\mu\mathbb{B}\rangle)\langle u^\mu u^\nu\rangle + \cdots,\end{aligned} \tag{17}$$

where $\chi_\pm = u^\dagger\chi u^\dagger \pm u\chi^\dagger u, \chi = 2B_0\mathcal{M}$ with B_0 a constant related to the quark condensate in the chiral limit and $\mathcal{M}$ the light-quark mass matrix. We will use the values of involved LECs from fit II in Ref. [48], which are $D = 0.8$, $F = 0.46$, $b_D = 0.222(20)$, $b_F = -0.428(12)$, $b_0 = -0.714(21)$, $b_1 = 0.515(132)$, $b_2 = 0.148(48)$, $b_3 = -0.663(155)$, $b_4 = -0.868(105)$, $b_5 = -0.643(246)$, $b_6 = -0.268(334)$, $b_7 = 0.176(72)$, $b_8 = -0.0694(1638)$.

3. The partial-wave amplitudes

Using the LO and NLO Lagrangians given in Eqs. (13) and (17), we can calculate the tree-level amplitude for the process of $\mathbb{B}\bar{\mathbb{B}} \to \pi\pi$ as depicted in Fig. 2. However, in order to determine the final state $\pi\pi$ with $IJ = 00$, we need to perform a partial-wave (PW) expansion. The generalized PW expansion of the helicity amplitude for arbitrary spin can be found in Ref. [49]. The final PW amplitude for $\mathbb{B}\bar{\mathbb{B}} \to \pi\pi$ reads

$$\begin{aligned}T_{\mathbb{B}\bar{\mathbb{B}}\to\pi\pi,L}(s) = {} & \frac{1}{4\pi}\int d\Omega\sqrt{\frac{4\pi}{2L+1}}Y^*_{L,\lambda_1-\lambda_2}(\theta,\phi) \\ & \times e^{i(\lambda_1-\lambda_2)\phi}\langle\theta,0;0,0|\hat{T}|0,0;\lambda_1,\lambda_2\rangle,\end{aligned} \tag{18}$$

where L is the relative orbital angular momentum of the pions, λ_1 and λ_2 are the third components of the helicities of $\mathbb{B}$ and $\bar{\mathbb{B}}$. The basis is such that $\mathbb{B}\bar{\mathbb{B}}$ is expanded in terms of $|\theta_0,\phi_0;\lambda_1,\lambda_2\rangle$, and the $\mathbb{B}\bar{\mathbb{B}}$ relative momentum is chosen to be along the z axis so that $\theta_0 = \phi_0 = 0$; (θ,ϕ) are the polar and azimuthal angles of the $\pi\pi$ relative momentum.

For the tree-level S-wave amplitude for $\mathbb{B}\bar{\mathbb{B}} \to \pi\pi$, the LHC part from the t- and u-channel baryon exchange is[5]

$$\hat{A}^N_0(s) = -\frac{\sqrt{3}(D+F)^2 m_N}{F_\pi^2}\frac{L(s,m_N,m_N,M_\pi)}{\sqrt{s-4m_N^2}}, \tag{19}$$

[4]Here we use the Lagrangian in [46] while the one in Ref. [45] has redundant terms. Note also that the ordering of the operators in Ref. [46] is different from that in Refs. [45,47].

[5]Here we consider only the baryon exchanges such that the two mesons emitted are two pions since we focus on the correlated S-wave two-pion exchange. That is, although we use an SU(3) chiral Lagrangian, the exchanged baryon has the same strangeness as the external ones. The framework may be understood as an SU(2) one for each of the baryons, but with the LECs matched to those in the SU(3) Lagrangian.

$$\hat{A}_0^{\Sigma}(s) = -\frac{4\sqrt{2}F^2 m_\Sigma}{F_\pi^2}\frac{L(s,m_\Sigma,m_\Sigma,M_\pi)}{\sqrt{s-4m_\Sigma^2}} - \frac{\sqrt{2}D^2(m_\Sigma+m_\Lambda)}{3F_\pi^2}\frac{L(s,m_\Sigma,m_\Lambda,M_\pi)}{\sqrt{s-4m_\Sigma^2}}, \tag{20}$$

$$\hat{A}_0^{\Lambda}(s) = \sqrt{\frac{2}{3}}\frac{D^2(m_\Lambda+m_\Sigma)}{F_\pi^2}\frac{L(s,m_\Lambda,m_\Sigma,M_\pi)}{\sqrt{s-4m_\Lambda^2}}, \tag{21}$$

$$\hat{A}_0^{\Xi}(s) = \frac{\sqrt{3}(D-F)^2 m_\Xi}{F_\pi^2}\frac{L(s,m_\Xi,m_\Xi,M_\pi)}{\sqrt{s-4m_\Xi^2}}, \tag{22}$$

where

$$\begin{aligned}
L(s,m_1,m_2,m) &= s - 2m_1(m_1-m_2) + H_0(s,m_1,m_2,m)H_1(s,m_1,m_2,m),\\
H_0(s,m_1,m_2,m) &= 2(m_1+m_2)[-2m^2m_1 + 2m_1(m_1-m_2)^2 + m_2 s],\\
H_1(s,m_1,m_2,m) &= \frac{H_2^+(s,m_1,m_2,m) - H_2^-(s,m_1,m_2,m)}{2\sqrt{(s-4m^2)(s-4m_1^2)}},\\
H_2^{\pm}(s,m_1,m_2,m) &= \ln\left[s - 2(m^2+m_1^2-m_2^2) \mp \sqrt{(s-4m^2)(s-4m_1^2)}\right].
\end{aligned}$$

The contact terms, which are from the NLO Lagrangian and contribute to the right-hand cut (RHC) part of $T_{\mathbb{B}\bar{\mathbb{B}}\to\pi\pi,0}(s)$ after taking into account the $\pi\pi$ rescattering, read

$$\begin{aligned}
A_0^N(s) = &\frac{\sqrt{s-4m_N^2}}{4\sqrt{3}F_\pi^2}(8M_\pi^2(6b_0 - 3(b_1+b_2+b_3+2b_4-b_D-b_F) - 2(b_5+b_6+b_7+2b_8)m_N)\\
&+ 4(3(b_1+b_2+b_3+2b_4) + (b_5+b_6+b_7+2b_8)m_N)s),
\end{aligned} \tag{23}$$

$$\begin{aligned}
A_0^\Sigma(s) = &\frac{\sqrt{s-4m_\Sigma^2}}{6\sqrt{2}F_\pi^2}(8M_\pi^2(9b_0 - 12b_1 - 6b_2 - 9b_4 + 9b_D - 2(4b_5+2b_7+3b_8)m_\Sigma)\\
&+ 4(12b_1 + 6b_2 + 9b_4 + 4b_5 m_\Sigma + 2b_7 m_\Sigma + 3b_8 m_\Sigma)s),
\end{aligned} \tag{24}$$

$$A_0^\Lambda(s) = -\frac{\sqrt{s-4m_\Lambda^2}}{6\sqrt{6}F_\pi^2}(8M_\pi^2(9b_0 - 6b_2 - 9b_4 + 3b_D - 4b_7 m_\Lambda - 6b_8 m_\Lambda) + 4(6b_2 + 9b_4 + 2b_7 m_\Lambda + 3b_8 m_\Lambda)s), \tag{25}$$

$$\begin{aligned}
A_0^\Xi(s) = &-\frac{\sqrt{s-4m_\Xi^2}}{4\sqrt{3}F_\pi^2}(8M_\pi^2(6b_0 - 3(b_1+b_2-b_3+2b_4-b_D+b_F) - 2(b_5-b_6+b_7+2b_8)m_\Xi)\\
&+ 4(3(b_1+b_2-b_3+2b_4) + (b_5-b_6+b_7+2b_8)m_\Xi)s),
\end{aligned} \tag{26}$$

where the parameter F_π is the decay constant of the π in the chiral limit. Since we use the LECs determined in Ref. [48], we adopt the same value $F_\pi = 87.1$ MeV [50] for consistency.

Moreover, employing Eq. (5), the tree-level S-wave amplitudes for $\mathbb{B}\bar{\mathbb{B}} \to \pi\pi$ after eliminating the kinematical singularities read, for the LHC part,

$$\hat{A}_0^{N\,\mathrm{new}}(s) = -\frac{\sqrt{3}(D+F)^2 m_N}{F_\pi^2}L(s,m_N,m_N,M_\pi), \tag{27}$$

$$\hat{A}_0^{\Sigma\,\mathrm{new}}(s) = -\frac{4\sqrt{2}F^2 m_\Sigma}{F_\pi^2}L(s,m_\Sigma,m_\Sigma,M_\pi) - \frac{\sqrt{2}D^2(m_\Sigma+m_\Lambda)}{3F_\pi^2}L(s,m_\Sigma,m_\Lambda,M_\pi), \tag{28}$$

$$\hat{A}_0^{\Lambda\,\mathrm{new}}(s) = \sqrt{\frac{2}{3}}\frac{D^2(m_\Lambda+m_\Sigma)}{F_\pi^2}L(s,m_\Lambda,m_\Sigma,M_\pi), \tag{29}$$

$$\hat{A}_0^{\Xi\,\mathrm{new}}(s) = \frac{\sqrt{3}(D-F)^2 m_\Xi}{F_\pi^2}L(s,m_\Xi,m_\Xi,M_\pi), \tag{30}$$

and for the contact term part,

$$A_0^{N\,\mathrm{new}}(s) = \frac{s-4m_N^2}{4\sqrt{3}F_\pi^2}(8M_\pi^2[6b_0 - 3(b_1+b_2+b_3+2b_4-b_D-b_F) - 2(b_5+b_6+b_7+2b_8)m_N] + 4[3(b_1+b_2+b_3+2b_4) + (b_5+b_6+b_7+2b_8)m_N]s), \tag{31}$$

$$A_0^{\Sigma\,\mathrm{new}}(s) = \frac{s-4m_\Sigma^2}{6\sqrt{2}F_\pi^2}(8M_\pi^2[9b_0 - 12b_1 - 6b_2 - 9b_4 + 9b_D - 2(4b_5+2b_7+3b_8)m_\Sigma] + 4(12b_1+6b_2+9b_4+4b_5m_\Sigma+2b_7m_\Sigma+3b_8m_\Sigma)s), \tag{32}$$

$$A_0^{\Lambda\,\mathrm{new}}(s) = -\frac{s-4m_\Lambda^2}{6\sqrt{6}F_\pi^2}(8M_\pi^2(9b_0 - 6b_2 - 9b_4 + 3b_D - 4b_7m_\Lambda - 6b_8m_\Lambda) + 4(6b_2+9b_4+2b_7m_\Lambda+3b_8m_\Lambda)s), \tag{33}$$

$$A_0^{\Xi\,\mathrm{new}}(s) = -\frac{s-4m_\Xi^2}{4\sqrt{3}F_\pi^2}(8M_\pi^2[6b_0 - 3(b_1+b_2-b_3+2b_4-b_D+b_F) - 2(b_5-b_6+b_7+2b_8)m_\Xi] + 4[3(b_1+b_2-b_3+2b_4) + (b_5-b_6+b_7+2b_8)m_\Xi]s). \tag{34}$$

4. The Muskhelishvili-Omnès representation

We now incorporate the $\pi\pi$ rescattering based on the tree-level amplitude, into the Muskhelishvili-Omnès representation. For the $\mathbb{B}\bar{\mathbb{B}} \to \pi\pi$ process, we partition the total S-wave kinematical-singularity-free amplitude into the LHC and the RHC parts,

$$T^{\mathrm{new}}_{\mathbb{B}\bar{\mathbb{B}}\to\pi\pi,0}(s) = R^{\mathrm{new}}_{\mathbb{B},0}(s) + L^{\mathrm{new}}_{\mathbb{B},0}(s). \tag{35}$$

Utilizing the $\pi\pi$ amplitude in the scalar-isoscalar channel $T_{\pi\pi\to\pi\pi,0}(s) = e^{i\delta_0(s)}\sin\delta_0(s)/\rho_\pi(s)$, where $\delta_0(s)$ is the S-wave isoscalar phase shift, and since there is no overlap between the LHC and RHC for kinematic-singularity-free amplitudes,[6] the unitary relation implies,

$$\mathrm{disc}[R^{\mathrm{new}}_{\mathbb{B},0}(s)] = 2i(R^{\mathrm{new}}_{\mathbb{B},0}(s) + L^{\mathrm{new}}_{\mathbb{B},0}(s)) \times e^{-i\delta_0(s)}\sin\delta_0(s)\theta(\sqrt{s}-2M_\pi). \tag{36}$$

To solve this equation, we first define the Omnès function [51],

$$\Omega_0(s) \equiv \exp\left[\frac{s}{\pi}\int_{4M_\pi^2}^{+\infty}\frac{\delta_0(z)}{z(z-s)}\mathrm{d}z\right]. \tag{37}$$

By using $\Omega_0(s\pm i\epsilon) = |\Omega_0(s)|e^{\pm i\delta_0(s)}$, we further derive

$$\mathrm{disc}\left[\frac{R^{\mathrm{new}}_{\mathbb{B},0}(s)}{\Omega_0(s)}\right] = 2i\frac{L^{\mathrm{new}}_{\mathbb{B},0}(s)}{|\Omega_0(s)|}\sin\delta_0(s)\theta(\sqrt{s}-2M_\pi). \tag{38}$$

[6]The RHC is chosen to be along the positive s axis in the interval $s \geq 4M_\pi^2$. The LHC is in the interval $(-\infty, (4m_{\mathbb{B}}^2M_\pi^2 - (m_0^2 - m_{\mathbb{B}}^2 - M_\pi^2)^2)/m_0^2]$ for the t- or u-channel process of $\mathbb{B}\bar{\mathbb{B}} \to \pi\pi$, where m_0 represents the mass of the exchanged particle. It can be easily proven that $(4m_{\mathbb{B}}^2M_\pi^2 - (m_0^2 - m_{\mathbb{B}}^2 - M_\pi^2)^2)/m_0^2 \leq 4M_\pi^2$.

Therefore, we can derive a DR with n subtractions,

$$R^{\mathrm{new}}_{\mathbb{B},0}(s) = \Omega_0(s)\left(P_{n-1}(s) + \frac{s^n}{\pi}\int_{4M_\pi^2}^{+\infty}\mathrm{d}z\frac{L^{\mathrm{new}}_{\mathbb{B},0}(z)\sin\delta_0(z)}{(z-s)z^n|\Omega_0(z)|}\right), \tag{39}$$

where $P_{n-1}(s)$ is an arbitrary polynomial of order $n-1$. Finally, we obtain a DR for $T^{\mathrm{new}}_{\mathbb{B}\bar{\mathbb{B}}\to\pi\pi,0}(s)$ as

$$T^{\mathrm{new}}_{\mathbb{B}\bar{\mathbb{B}}\to\pi\pi,0}(s) = L^{\mathrm{new}}_{\mathbb{B},0}(s) + \Omega_0(s)\left(P_{n-1}(s) + \frac{s^n}{\pi}\int_{4M_\pi^2}^{+\infty}\mathrm{d}z\frac{L^{\mathrm{new}}_{\mathbb{B},0}(z)\sin\delta_0(z)}{(z-s)z^n|\Omega_0(z)|}\right). \tag{40}$$

For the phase shift $\delta_0(s)$, we take the parametrization in Ref. [52]. For the $\Omega_0(s)$ Omnès function, we take the $\Omega_{11}(s)$ matrix element of the coupled-channel Omnès matrix for the $\pi\pi - K\bar{K}$ S-wave interaction obtained in Ref. [53].

The above equation provides a reasonable form that incorporates the $\pi\pi$ rescattering. The LHC part $L^{\mathrm{new}}_{\mathbb{B},0}(s)$ and the polynomial $P_{n-1}(s)$ may be determined by matching at low energies to the chiral amplitudes as done in Refs. [54–58]. We perform the matching when the $\pi\pi$ rescattering is switched off, i.e., $\delta_0(s) = 0$, which leads to $\Omega_0(s) = 1$. Consequently, for the $\mathbb{B}\bar{\mathbb{B}} \to \pi\pi$ process, we can approximate $L^{\mathrm{new}}_{\mathbb{B},0}(s) \sim \hat{A}_0^{\mathbb{B}\,\mathrm{new}}(s)$ and $P_{n-1}(s) \sim A_0^{\mathbb{B}\,\mathrm{new}}(s)$.

Moreover, there is a polynomial ambiguity as discussed in Refs. [59,60]. If the asymptotic value of the phase shift $\delta_0(s)$ is not 0 but $n\pi$ as $s \to \infty$, the corresponding Omnès function will approach $1/s^n$ asymptotically. In our case, the phase shift $\delta_0(s) \overset{s\to\infty}{\to} \pi$ implies $\Omega_0(s) \overset{s\to\infty}{\to} 1/s$, thus the general solution of the unitarity condition (36) contains

three free parameters [59,60] (assuming that $T^{\rm new}_{\mathbb{B}\bar{\mathbb{B}}\to\pi\pi,0}$ is asymptotically bounded by s). However, although the standard twice subtracted DR via Eq. (40) indeed grows like s (notice that $n=2$), it contains only two free parameters in the polynomial, i.e., one parameter less than the general solution. Hence we propose an oversubtracted DR (twice subtracted DR with an order-2 polynomial matching to the ChPT amplitudes) that can be solved uniquely. In summary, the final DR is given as

$$T^{\rm new}_{\mathbb{B}\bar{\mathbb{B}}\to\pi\pi,0}(s)=\hat{A}_0^{\mathbb{B}\,\rm new}(s)+\Omega_0(s)\left(A_0^{\mathbb{B}\,\rm new}(s)+\frac{s^2}{\pi}\int_{4M_\pi^2}^{+\infty}\mathrm{d}z\frac{\hat{A}_0^{\mathbb{B}\,\rm new}(z)\sin\delta_0(z)}{(z-s)z^2|\Omega_0(z)|}\right). \tag{41}$$

From the above derivation, it is important to note that Eq. (41) can only be applied when the singularity of the LHC is exclusively included in $\hat{A}_0^{\mathbb{B}\,\rm new}(s)$, and there is no overlap between the LHC and RHC. The original t- and u-channel exchange amplitudes Eqs. (19)–(22) do not satisfy this condition due to the factor $\sqrt{s-4m_{\mathbb{B}}^2}$. Let us take $\Sigma\bar{\Sigma}\to\pi\pi$ as an example. From Fig. 3, it becomes apparent that the amplitude in Eq. (20) includes the LHC $(-\infty,4M_\pi^2-M_\pi^4/m_\Sigma^2]$ derived from the particle exchanging in the crossed channel, as well as a kinematical cut in the physical region. Therefore, directly substituting Eq. (20) into Eq. (41) is invalid and disrupts the self-consistency of the theory. By employing the method described in Sec. II B 1 to eliminate the kinematical singularities, the kinematical-singularity-free S-wave amplitude $\hat{A}_0^{\Sigma\,\rm new}(s)$ in Eq. (28) has only the LHC and satisfies the condition for Eq. (41), as demonstrated in Fig. 4.

At this stage, we can substitute the amplitude given by Eqs. (27)–(34) into Eq. (41) to obtain the amplitude denoted as $T^{\rm new}_{\mathbb{B}\bar{\mathbb{B}}\to\pi\pi,0}(s)$. It includes the S-wave $\pi\pi$ rescattering and does not exhibit any kinematical singularities. Then, utilizing Eqs. (9)–(12), we get the discontinuity in Eq. (4), and finally, the DR amplitude for $\mathbb{B}\bar{\mathbb{B}}\to\bar{\mathbb{B}}\mathbb{B}$ from exchanging correlated S-wave $\pi\pi$ is obtained by performing the dispersive integral.

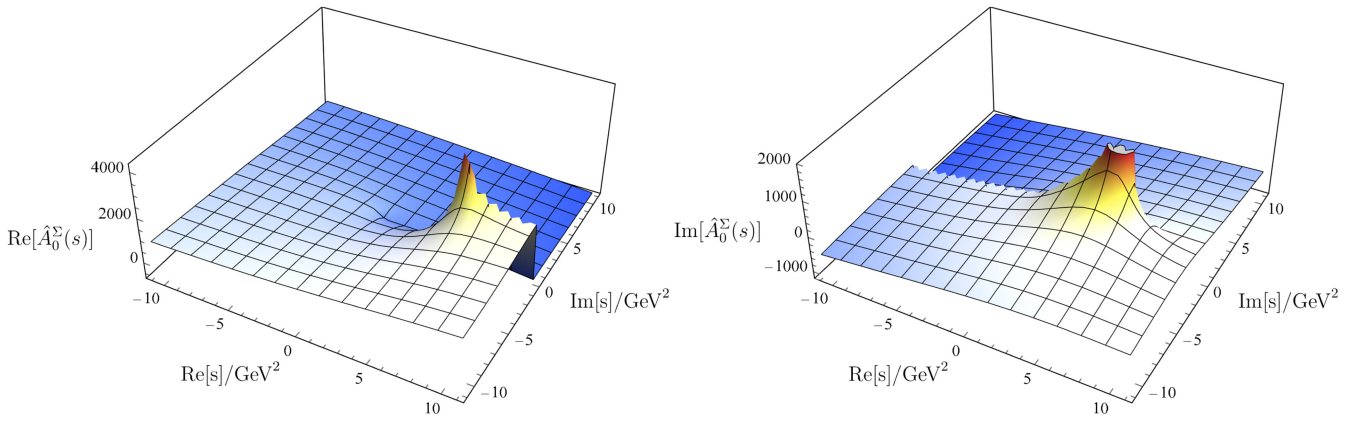

FIG. 3. Real (left panel) and imaginary (right panel) parts of the tree-level t- and u-channel exchange amplitude for the process of $\Sigma\bar{\Sigma}\to\pi\pi$ projected to the $\pi\pi$ S-wave as given in Eq. (20). The branch cut of the square root function is chosen to be along the positive real s axis.

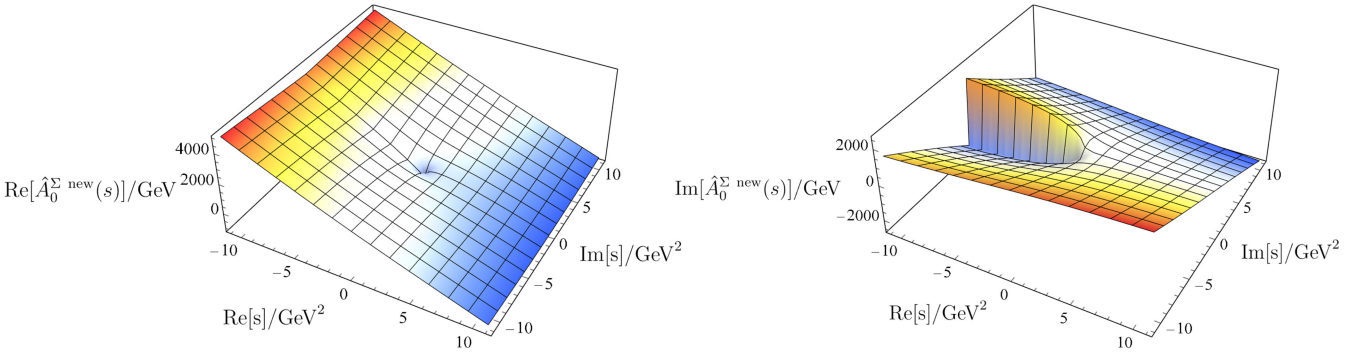

FIG. 4. Real (left panel) and imaginary (right panel) parts of the tree-level t- and u-channel exchange amplitude as given in Eq. (28) for the process of $\Sigma\bar{\Sigma}\to\pi\pi$ projected to the $\pi\pi$ S-wave. The amplitude is free of kinematical singularities and has only the desired LHC.

III. DETERMINATION OF COUPLING CONSTANTS

Now we compare the two amplitudes, $\mathcal{M}^{\rm OBE}$ in Eq. (3) and $\mathcal{M}^{\rm DR}$ and Eq. (4), to determine the coupling constant $g_{\mathbb{B}\mathbb{B}\sigma}$.

A. Matching s-channel amplitudes

Let us first compare the two amplitudes in Eqs. (3) and (4) in the s-channel physical region, specifically $s \geq 4m_{\mathbb{B}}^2$. Since the amplitudes from exchanging σ and

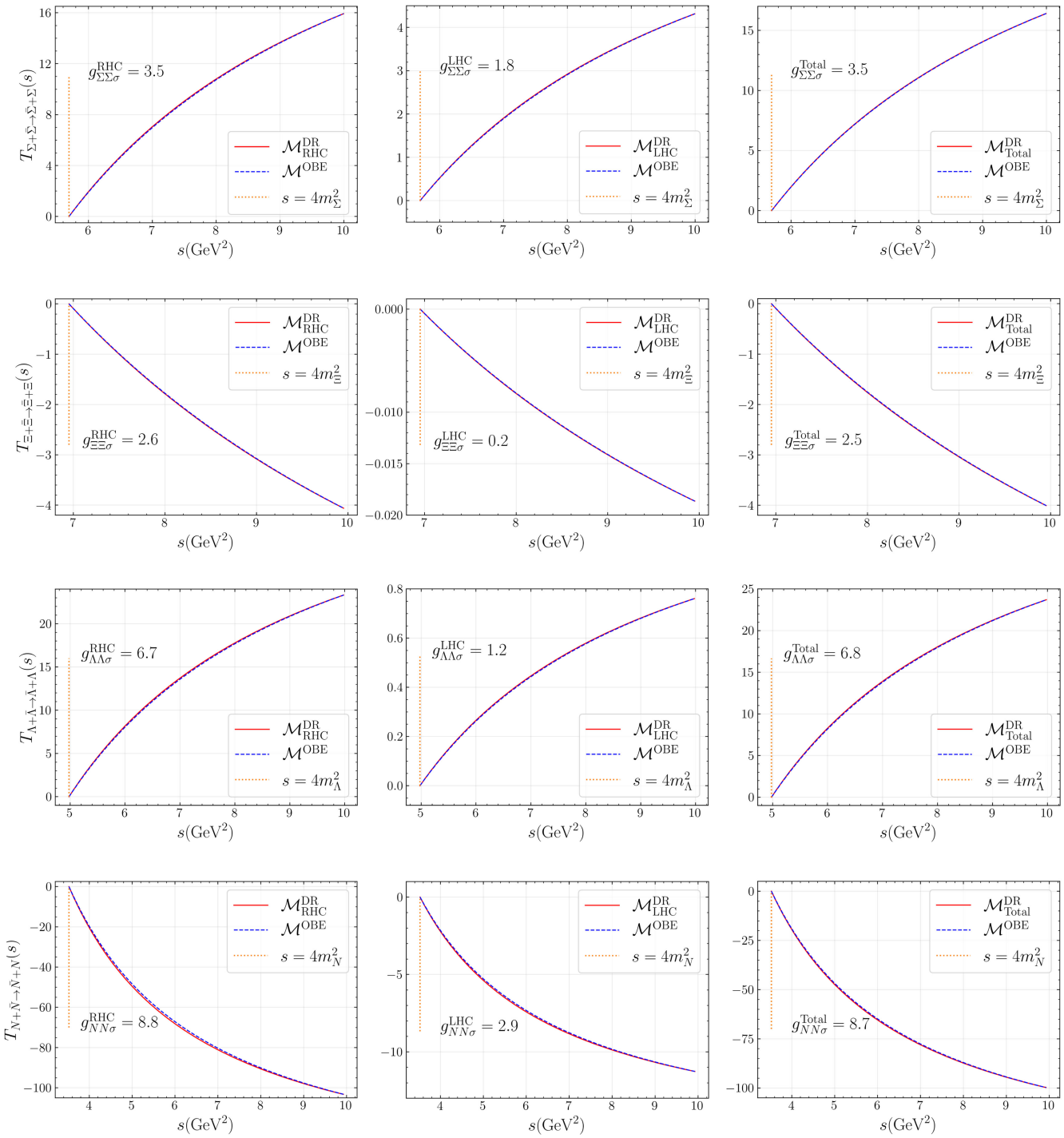

FIG. 5. Comparison of the OBE amplitudes with different coupling constants obtained from s-channel σ exchange and the DR amplitudes for different cases by using the central values of the LECs provided in Ref. [48] and setting $\sqrt{s_0}$ to 0.8 GeV as in Ref. [39]. The subscripts RHC, LHC, and Total in $\mathcal{M}^{\rm DR}$ represent that the corresponding amplitudes consider only the RHC part shown in Fig. 2(c), only the LHC part shown in Figs. 2(a) and 2(b), and both contributions combined, respectively.

TABLE I. The coupling constants $g_{\mathbb{B}\mathbb{B}\sigma}$ as given by the sum rule in Eq. (43).[a] The second, third and fourth columns list the results when only the LHC part shown in Figs. 2(a) and 2(b), only the RHC part shown in Fig. 2(c) and both of them are considered, respectively. The fifth to eleventh columns list the coupling constants from other references. For the seventh column, the values outside and inside the brackets represent the results calculated using different models in Ref. [34]. The last column lists the mass (in MeV) of the σ determined in the t/u-channel amplitude matching, as detailed in Sec. III B. The last row for $g^{\mathrm{SU(2)}}_{NN\sigma}$ lists the results obtained in the SU(2) framework, as detailed in Appendix B.

	LHC	RHC	Total	[33]	[18]	[34]	[37]	[36]	[24]	[23]	m_σ
$g_{\Sigma\Sigma\sigma}$	$1.8^{+0.5}_{-0.5}$	$3.5^{+2.0+0.8}_{-1.8-0.9}$	$3.5^{+1.8+0.4}_{-1.3-0.4}$	⋯	⋯	10.85(8.92)	4.65	⋯	⋯	⋯	519^{+50}_{-48}
$g_{\Xi\Xi\sigma}$	$0.2^{+0.1}_{-0.1}$	$2.6^{+1.5+0.5}_{-1.4-0.6}$	$2.5^{+1.5+0.5}_{-1.3-0.6}$	⋯	⋯	⋯	⋯	⋯	3.4	⋯	614^{+56}_{-81}
$g_{\Lambda\Lambda\sigma}$	$1.2^{+0.4}_{-0.3}$	$6.7^{+1.0+1.4}_{-1.1-1.7}$	$6.8^{+1.0+1.1}_{-1.0-1.4}$	⋯	⋯	8.18(6.54)	4.37	⋯	⋯	6.59	596^{+41}_{-51}
$g_{NN\sigma}$	$2.9^{+0.9}_{-0.8}$	$8.8^{+1.4+1.9}_{-1.4-2.3}$	$8.7^{+1.3+1.1}_{-1.3-1.4}$	12.78	8.46	8.46	8.58	13.85	10.2	9.86	558^{+33}_{-42}
$g^{\mathrm{SU(2)}}_{NN\sigma}$	$2.7^{+0.8}_{-0.8}$	$12.5^{+0.2+2.6}_{-0.2-3.2}$	$12.2^{+0.2+1.9}_{-0.2-2.3}$								586^{+38}_{-48}

[a]The numerical results show that the total coupling $g^{\mathrm{total}}_{\mathbb{B}\mathbb{B}\sigma}$ does not align with the mere addition of the LHC and RHC couplings, $g^{\mathrm{LHC}}_{\mathbb{B}\mathbb{B}\sigma}+g^{\mathrm{RHC}}_{\mathbb{B}\mathbb{B}\sigma}$. This difference stems from the fact that both the LHC and RHC terms in Eq. (41) share the same phase factor, specifically $e^{i\delta_0(s)}$. Consequently, we anticipate the emergence of constructive and destructive interference effects in the subsequent computations involving the squared amplitude, as detailed in Eqs. (9)–(12), as well as during the integration procedures outlined in Eq. (43).

from exchanging the correlated S-wave $\pi\pi$ have the same Lorentz structure, we can compare the two amplitudes at large s values so that the pion masses and the σ mass in the OBE amplitude play little role. A comparison of $\mathcal{M}^{\mathrm{OBE}}$ and $\mathcal{M}^{\mathrm{DR}}$ in the physical region of $s\geq 4m_{\mathbb{B}}^2$ is shown in Fig. 5, where $g_{\mathbb{B}\mathbb{B}\sigma}$ has been adjusted so that the two amplitudes coincide in the physical region and $m_\sigma=0.5$ GeV is taken. In fact, matching Eqs. (3) and (4) at $s\geq 4m_{\mathbb{B}}^2$, one gets

$$-2\pi i C_{\mathbb{B}} g^2_{\mathbb{B}\mathbb{B}\sigma}\approx\int_{4M_\pi^2}^{s_0}\frac{\mathrm{disc}[\mathcal{M}^{\mathrm{DR}}_{\mathbb{B}\bar{\mathbb{B}}\to\bar{\mathbb{B}}\mathbb{B},0}(z)]}{z-4m_{\mathbb{B}}^2}\frac{s-m_\sigma^2}{s-z}\mathrm{d}z. \quad (42)$$

Since s is much larger than both m_σ^2 or $z\leq s_0\simeq(0.8\ \mathrm{GeV})^2$, one obtains the following sum rule:

$$g^2_{\mathbb{B}\mathbb{B}\sigma}=-\frac{1}{2\pi i C_{\mathbb{B}}}\int_{4M_\pi^2}^{s_0}\frac{\mathrm{disc}[\mathcal{M}^{\mathrm{DR}}_{\mathbb{B}\bar{\mathbb{B}}\to\bar{\mathbb{B}}\mathbb{B},0}(z)]}{z-4m_{\mathbb{B}}^2}\mathrm{d}z. \quad (43)$$

The numerical results of the scalar coupling constants are presented in Table I, where the uncertainties in the second to fourth columns arise from the error propagated from those of the NLO LECs and the choice of the upper limit for the dispersive integral (see below), corresponding to Eqs. (4) and (41). In addition to the results obtained in the SU(3) framework, we also investigate $g_{NN\sigma}$ in the SU(2) framework. The details are presented in Appendix B, and the results are listed in the last row in Table I, labeled as $g^{\mathrm{SU(2)}}_{NN\sigma}$. Moreover, remarks are made on the difference in $g_{NN\sigma}$ under the SU(2) and SU(3) frameworks in Appendix B.

Let us comment on the calculation of the two dispersive integrals. The first one, given by Eq. (41), is computed over the integration range of $[4M_\pi^2,(\sqrt{s_0}+\epsilon)^2]$. The second one, given by Eq. (4), is integrated over $[(2M_\pi+\epsilon)^2,s_0]$.[8] Note that the range of the second integral is completely covered by that of the first one to avoid unphysical singularities.

The central values in Table I are obtained by setting $\sqrt{s_0}$ to 0.8 GeV as in Ref. [39] and utilizing the central values of the NLO LECs provided in Ref. [48]. The uncertainties of the NLO LECs as determined in Ref. [48] are propagated to the coupling constants by using the bootstrap method. The resulting average values and corresponding standard deviations introduce the first source of errors in the third and fourth columns in Table I (the b_i LECs appear only in the RHC contributions, and we have fixed the pion decay constant; thus the second column does not have errors from LECs). Furthermore, we vary $\sqrt{s_0}$ from 0.7 to 0.9 GeV, which constitute the errors in the second column and the second source of errors in the third and fourth columns.

Results from other studies on these scalar couplings are also listed in Table I. For $g_{NN\sigma}$ that has been estimated in many works, we find a good agreement with existing results, which supports the validity of our framework. Here we briefly discuss the methods used in the literature. In Ref. [33], the authors investigated the S-wave $N\bar{N}\to\pi\pi$ amplitudes with the $\pi\pi$ rescattering and the results revealed that the intertwined contribution from the $\pi\pi$ S-wave can be elegantly described as a broad σ meson with a mass of approximately $m_\sigma\sim 4.8M_\pi$ and a coupling strength of $g_{NN\sigma}\sim 12.78$. In Ref. [18], displaying the outcomes derived from the Bonn meson-exchange model, they found that the correlated S-wave $\pi\pi$ exchange can be further

[8]Here, ϵ represents a small positive quantity that is relatively insignificant when compared to $\sqrt{s_0}$ and $2M_\pi$. As long as it is much smaller than M_π, the specific value has negligible impact on the results.

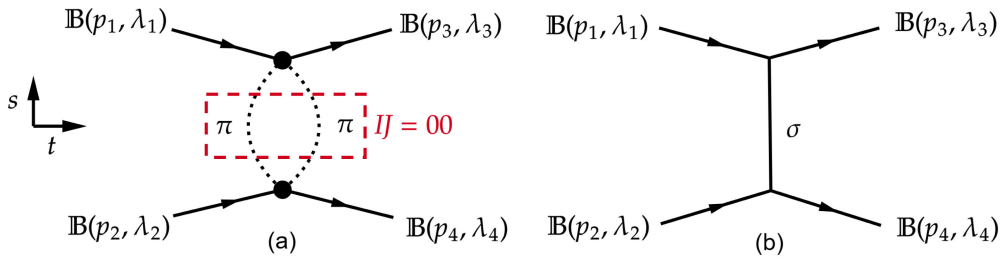

FIG. 6. The Feynman diagram for the t-channel process of $\mathbb{B}\mathbb{B} \to \mathbb{B}\mathbb{B}$ with the intermediate state of $\pi\pi$ (a) or σ (b). In (a), the black dots imply $\pi\pi$ interaction.

approximated by a zero width scalar exchange, with the corresponding mass and coupling constant readjusted to 550 MeV and 8.46, respectively. In Ref. [34], the authors also considered the σ exchange as an effective parameterization for the correlated S-wave $\pi\pi$ exchange contribution. They utilized the result from the full Bonn meson-exchange model [18] for the nucleon, i.e., the value in the sixth column of Table I, and $g_{\Lambda\Lambda\sigma}$ and $g_{\Sigma\Sigma\sigma}$ are determined by a fit to the empirical hyperon-nucleon data using two different models, with the distinction lying in whether higher-order processes involving a spin-$\frac{3}{2}$ baryon in the intermediate state were considered in the hyperon-nucleon interaction. In Ref. [37], the authors calculated the $\mathbb{B}\bar{\mathbb{B}}' \to \pi\pi$ and $\mathbb{B}\bar{\mathbb{B}}' \to K\bar{K}$ amplitudes in the light of hadron-exchange picture. Based on an ansatz for Lagrangian, various symmetries and assumptions, they reduced the number of free parameters as many as possible, and then the parameters were fixed by adjusting the $N\bar{N} \to \pi\pi$ amplitudes to the quasiempirical data. With these parameters and the existing $\pi\pi$ scattering phase shifts they got the $\mathbb{B}\bar{\mathbb{B}}' \to \pi\pi$ and $\mathbb{B}\bar{\mathbb{B}}' \to K\bar{K}$ amplitudes in the pseudophysical region after solving the Blankenbecler-Sugar equation. Then employing the DR they got the spectral function that denotes the strength of a hadron-exchange process, namely the coupling constants. The eighth column in Table I represents their results, which are also similar to those reported in Ref. [38]. In later development of the Jülich meson-exchange model in Ref. [36], the authors conducted an analysis of the coupled-channel dynamics and performed a simultaneous fit to the experimental data of various reactions, including $\pi N \to \pi N$, ηN, $K\Lambda$, and $K\Sigma$, with the $\pi\pi N$ intermediate state parameterized as the σN, $\pi\Delta$, and ρN channels. In their fitting, the coupling constant is determined to be $g_{NN\sigma} = 13.85$. In Ref. [23], the authors used $g_{\Lambda\Lambda\sigma} = \frac{2}{3} g_{NN\sigma}$ from SU(3) consideration and took $g_{NN\sigma}$ from Ref. [18]. In Ref. [24], $g_{NN\sigma} = m_N/F_\pi$ was determined using the linear σ model [61]. Then under the assumption that the σ meson only couples to the u and d quarks, the authors got $g_{\Xi\Xi\sigma} = \frac{1}{3} g_{NN\sigma}$ based on the quark model consideration. Additionally, in Ref. [62], the authors calculated the NN potential arising from the exchange of a correlated S-wave isoscalar pion pair, i.e., the σ channel, utilizing a unitary approach based on the lowest order chiral Lagrangian and the Bethe-Salpeter equation for the analysis of $\pi\pi$ scattering. A qualitative estimate for $g_{NN\sigma} \sim 5$ was obtained, at the right order of the values quoted in Table I.

B. Matching t/u-channel amplitudes

In the preceding subsection, it becomes evident that for the s-channel process of $\mathbb{B}\bar{\mathbb{B}} \to \bar{\mathbb{B}}\mathbb{B}$, the selection of an apt coupling constant $g_{\mathbb{B}\mathbb{B}\sigma}$ allows for the σ exchange to mimic the correlated $\pi\pi$ intermediate state with $IJ = 00$ in physical region, $s \geq 4m_{\mathbb{B}}^2$. However, when employing the OBE model to estimate the interaction between hadrons, the σ is exchanged in the t or u channel, as illustrated in Fig. 6(b) rather than in the s-channel, as demonstrated in Fig. 1(b). Therefore, to derive the parameters for the σ exchange that can be used in the OBE model, one needs to conduct an analysis of the t- and u-channel meson-exchange processes. As elaborated in Appendix C, the crossing symmetry relations provide a means to relate the $t(u)$-channel process to the s-channel one. It becomes evident that, should we manage to align the two amplitudes within the nonphysical region of the s-channel process, specifically $s \in [4m_{\mathbb{B}}^2 - t, 0]$, we can subsequently match the corresponding pair of amplitudes within the physical region of the $t(u)$-channel process, i.e., $t \geq 4m_{\mathbb{B}}^2$, relevant for the low-energy $\mathbb{B}\mathbb{B}$ scattering.

In order for the σ exchange to approximate the S-wave correlated two pions in the few hundred MeV region, we also need to adjust the σ mass in addition to the couplings derived above.[9] As an example, in Fig. 7, we show the comparison of the OBE amplitude and the DR amplitude for the $\Xi\Xi$ case at the t-channel threshold. One finds from Fig. 7(b) that by adjusting the σ mass to about 614^{+56}_{-81} MeV, the DR amplitude using the central values of the LECs can be very well reproduced. The matching point has been chosen to be $s = 0$ GeV^2, corresponding to the t-channel $\mathbb{B}\mathbb{B}$ threshold. To see the dependence on the σ mass, we also show the comparison for $m_\sigma = 500$ MeV in Fig. 7(a).

[9]Since in the $\mathbb{B}\mathbb{B}$ scattering physical region, the exchanged two pions cannot go on shell, a real mass, instead of the complex pole, for the σ meson in the OBE model should be used.

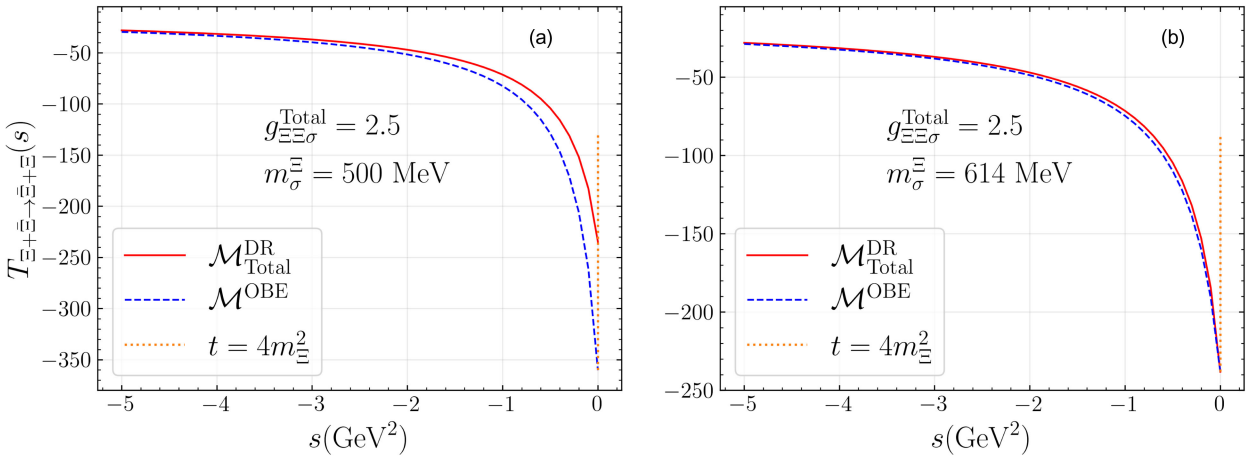

FIG. 7. Comparison of the OBE amplitude, with the coupling constant taking the central value listed in Table I and different m^{Ξ}_{σ} values in the process of $\Xi\bar{\Xi} \to \bar{\Xi}\Xi$, and the DR amplitude using the central values of the LECs provided in Ref. [48] and setting $\sqrt{s_0}$ to 0.8 GeV as in Ref. [39].

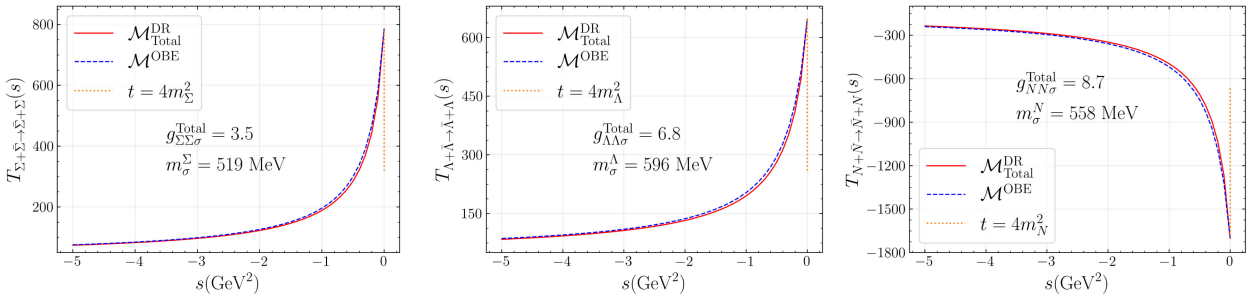

FIG. 8. Matching at $\mathbb{B}\mathbb{B}$ threshold the OBE amplitudes, with the coupling constant taking the central value listed in Table I, to the DR amplitudes using the central values of the LECs provided in Ref. [48] and setting $\sqrt{s_0}$ to 0.8 GeV as in Ref. [39].

The aforementioned analysis can be readily extended to the other ground state octet baryons, yielding the results shown in Fig. 8. From Figs. 5, 7(b), and 8, it is apparent that if our aim is to use a simple σ exchange in the OBE model to concurrently match a complex correlated $\pi\pi$ exchange with $IJ = 00$ in the s-, t- and u-channel physical region, the m_{σ} values required by different processes differ. Specifically, we find $m^{\Sigma}_{\sigma} = 519^{+50}_{-48}$ MeV, $m^{\Xi}_{\sigma} = 614^{+56}_{-81}$ MeV, $m^{\Lambda}_{\sigma} = 596^{+41}_{-51}$ MeV, and $m^{N}_{\sigma} = 558^{+33}_{-42}$ MeV, where the uncertainties correspond to those of the couplings added in quadrature.[10] These values are listed in the last column of Table I. This echoes previous attempts to modify the mass of σ, a broad resonance with a mass approximately equal to $4.8M_{\pi}$ [33], to a mass of 550 MeV with a zero width [18], which is within all the above ranges. The goal of such modification was to allow a single σ exchange to more accurately replicate the results of a correlated $\pi\pi$ exchange with $IJ = 00$.

[10]The superscript of $m^{\mathbb{B}}_{\sigma}$ is utilized to represent the mass of this σ which is derived from the process of $\mathbb{B}\bar{\mathbb{B}} \to \bar{\mathbb{B}}\mathbb{B}$.

IV. SUMMARY

In this work, we evaluate the couplings of the σ meson to the $\frac{1}{2}^+$ ground state light baryons, which are essential inputs of the OBE models, by matching the baryon-baryon scattering amplitudes through correlated S-wave isoscalar $\pi\pi$ intermediate state to the OBE ones. Using the LO and NLO SU(3) chiral baryon-meson Lagrangians, we carefully handle the kinematical singularities and utilize DR and incorporate the $\pi\pi$ rescattering by Muskhelishvili-Omnès representation to obtain the DR amplitude. Considering the phenomenological σ exchange as an effective parametrization for the correlated $\pi\pi$ exchange contribution in the $IJ = 00$ channel, we determine the scalar coupling constants $g_{\mathbb{B}\mathbb{B}\sigma}$ from the s-channel matching, as listed in Table I. Specifically, $g_{\Sigma\Sigma\sigma} = 3.5^{+1.8}_{-1.3}$, $g_{\Xi\Xi\sigma} = 2.5^{+1.5}_{-1.4}$, $g_{\Lambda\Lambda\sigma} = 6.8^{+1.5}_{-1.7}$, and $g_{NN\sigma} = 8.7^{+1.7}_{-1.9}$, where the errors are obtained by adding the corresponding ones in Table I in quadrature. This is achieved by comparing the DR amplitude and OBE amplitude in the physical region of the s-channel process, specifically, $s \geq 4m^2_{\mathbb{B}}$. Concurrently, we estimate the uncertainties of the scalar coupling constants arising from the NLO LECs [48] and variation of the upper

limit for the dispersive integral. Moreover, by extending the analysis to the physical region of the corresponding t/u-channel process via the crossing relation, we obtain the σ mass to be used together with the determined $\mathbb{B}\mathbb{B}\sigma$ coupling constant. The value depends on the process but is always around 550 MeV. We also compute the $NN\sigma$ coupling by matching to the SU(2) ChPT amplitude with the LECs determined in Refs. [63,64], and the result is $g^{\mathrm{SU}(2)}_{NN\sigma} = 12.2^{+1.9}_{-2.3}$.

The effective coupling constants obtained here can be used to describe the interaction between light hadrons and other hadrons through the σ exchange. The same method can be applied to the determination of the coupling constants of σ and other hadrons, such as heavy mesons and baryons, the interactions between which are crucial to understand the abundance of exotic hadron candidates observed at various experiments in last two decades.

ACKNOWLEDGMENTS

We would like to thank Ulf-G. Meißner for a careful reading of the manuscript. This work is supported in part by the Chinese Academy of Sciences under Grants No. XDB34030000 and No. YSBR-101; by the National Natural Science Foundation of China (NSFC) and the Deutsche Forschungsgemeinschaft (DFG) through the funds provided to the Sino-German Collaborative Research Center TRR110 "Symmetries and the Emergence of Structure in QCD" (NSFC Grant No. 12070131001, DFG Project-ID 196253076); by the NSFC under Grants No. 12125507, No. 11835015, and No. 12047503; and by the Postdoctoral Fellowship Program of China Postdoctoral Science Foundation (CPSF) under Grant No. GZC20232773 and the CPSF Grant No. 2023M743601.

APPENDIX A: ISOSPIN CONVENTIONS

In this work, we use the following isospin conventions [65]:

$$
\begin{aligned}
|\pi^+\rangle &= -|1,1\rangle, & |\pi^0\rangle &= |1,0\rangle,\\
|\pi^-\rangle &= |1,-1\rangle, & |\Sigma^+\rangle &= -|1,1\rangle,\\
|\Sigma^0\rangle &= |1,0\rangle, & |\Sigma^-\rangle &= |1,-1\rangle,\\
|\bar{\Sigma}^+\rangle &= -|1,1\rangle, & |\bar{\Sigma}^0\rangle &= |1,0\rangle,\\
|\bar{\Sigma}^-\rangle &= |1,-1\rangle, & |\Xi^0\rangle &= \left|\frac{1}{2},\frac{1}{2}\right\rangle,\\
|\Xi^-\rangle &= \left|\frac{1}{2},-\frac{1}{2}\right\rangle, & |\bar{\Xi}^+\rangle &= -\left|\frac{1}{2},\frac{1}{2}\right\rangle,\\
|\bar{\Xi}^0\rangle &= \left|\frac{1}{2},-\frac{1}{2}\right\rangle, & |\Lambda^0\rangle &= |0,0\rangle,\\
|p\rangle &= \left|\frac{1}{2},\frac{1}{2}\right\rangle, & |n\rangle &= \left|\frac{1}{2},-\frac{1}{2}\right\rangle,\\
|\bar{n}\rangle &= \left|\frac{1}{2},\frac{1}{2}\right\rangle, & |\bar{p}\rangle &= -\left|\frac{1}{2},-\frac{1}{2}\right\rangle.
\end{aligned}
$$

Therefore, we can readily obtain the isoscalar state $|I=0, I_3=0\rangle$ composed of $\pi\pi$, $\mathbb{B}\bar{\mathbb{B}}$, and $\bar{\mathbb{B}}\mathbb{B}$ in the particle basis.

APPENDIX B: $g_{NN\sigma}$ FROM SU(2) AND ChPT

It is worth mentioning that in the context of πN interaction, it is more common to utilize the Lagrangian within the SU(2) framework, the LO Lagrangian is given by

$$
\mathcal{L}^{(1)}_{\pi N} = \bar{\Psi}\left(i\mathcal{D} - m_N + \frac{g_A}{2}\gamma^\mu\gamma_5 u_\mu\right)\Psi, \tag{B1}
$$

where g_A represents the nucleon axial-vector coupling constant in the chiral limit and is related to the SU(3) LECs via $g_A = D + F$. At the NLO,

$$
\begin{aligned}
\mathcal{L}^{(2)}_{\pi N} = {} & c_1\mathrm{Tr}(\chi_+)\bar{\Psi}\Psi - \frac{c_2}{4m_N^2}\mathrm{Tr}(u_\mu u_\nu)(\bar{\Psi}\mathcal{D}^\mu\mathcal{D}^\nu\Psi + \mathrm{H.c.})\\
& + \frac{c_3}{2}\mathrm{Tr}(u^\mu u_\mu)\bar{\Psi}\Psi - \frac{c_4}{4}\bar{\Psi}\gamma^\mu\gamma^\nu[u_\mu, u_\nu]\Psi\\
& + c_5\bar{\Psi}\left[\chi_+ - \frac{1}{2}\mathrm{Tr}(\chi_+)\right]\Psi\\
& + \bar{\Psi}\sigma^{\mu\nu}\left[\frac{c_6}{2}f^+_{\mu\nu} + \frac{c_7}{2}v^{(s)}_{\mu\nu}\right]\Psi,
\end{aligned} \tag{B2}
$$

which contains seven LECs c_i [66–69], the first four of which are determined in Refs. [63,64] as (in units of GeV^{-1}),

$$
\begin{aligned}
c_1 &= -0.74 \pm 0.02, & c_2 &= 1.81 \pm 0.03,\\
c_3 &= -3.61 \pm 0.05, & c_4 &= 2.17 \pm 0.03.
\end{aligned} \tag{B3}
$$

By utilizing the Eqs. (B1) and (B2) and the above LECs, we obtain the following results through the s-channel matching as detailed in Sec. III A:

$$
\begin{aligned}
g^{\mathrm{LHC}}_{NN\sigma} &= 2.7^{+0.8}_{-0.8}, & g^{\mathrm{RHC}}_{NN\sigma} &= 12.5^{+0.2+2.6}_{-0.2-3.2},\\
g^{\mathrm{Total}}_{NN\sigma} &= 12.2^{+0.2+1.9}_{-0.2-2.3}.
\end{aligned} \tag{B4}
$$

Notice that here for consistency with the c_i values, we take $F_\pi = 92.2$ MeV and $g_A = 1.2723$ used in Refs. [63,64], larger than the value used in the main text. Meanwhile, from matching the t/u-channel amplitudes, we find $m^{N\mathrm{SU}(2)}_\sigma = 586^{+38}_{-48}$ MeV. The $g^{\mathrm{Total}}_{NN\sigma}$ value given above is close to the real part of the coupling defined as the residue of the $\pi\pi \to N\bar{N}$ amplitude at the $f_0(500)$ pole obtained in Ref. [70], which is 12.1 ± 1.4.

As per Table I, the $g^{\mathrm{RHC}}_{NN\sigma}$ central value calculated using the ChPT NLO Lagrangian within the SU(2) framework deviates from its value within the SU(3) framework.

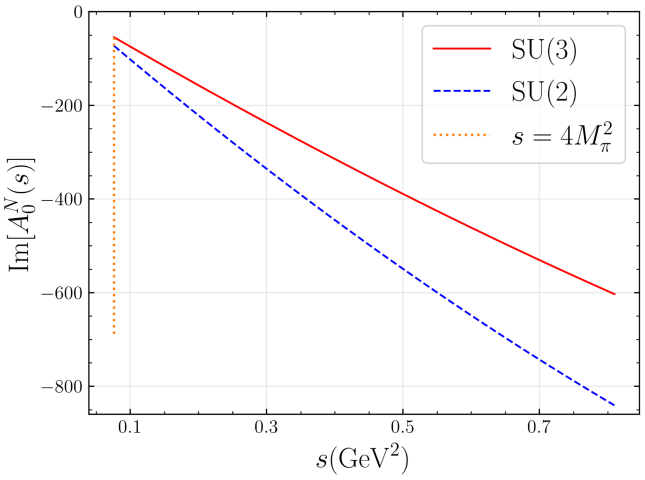

FIG. 9. The contact term amplitudes of the $N\bar{N} \to \pi\pi$ process derived from the SU(2) and SU(3) chiral Lagrangians using the central values of LECs determined in Refs. [48,63,64], respectively.

In Fig. 9, we show a comparison of the S-wave tree-level amplitudes of the contact terms for the $N\bar{N} \to \pi\pi$ process from the SU(3) chiral Lagrangian with that from the SU(2) chiral Lagrangian, the LECs of which are taken from Refs. [48] and [63,64], respectively. One sees a clear deviation. We have checked that the deviation from the SU(2) result would be larger if we use the central values of the SU(3) LECs determined by other groups [47,71–73]. Nevertheless, the values of $g_{NN\sigma}$ and $g_{NN\sigma}^{\mathrm{SU(2)}}$ from RHC contributions agree within uncertainties. One notices that Refs. [48,63,64] considered different experimental and lattice datasets.

APPENDIX C: THE CROSSING RELATION

Based on the crossing symmetry, we can establish a relation between the s-channel helicity amplitude of $\mathbb{B}\bar{\mathbb{B}} \to \bar{\mathbb{B}}\mathbb{B}$ and the t-channel helicity amplitude of $\mathbb{B}\mathbb{B} \to \mathbb{B}\mathbb{B}$ or the u-channel helicity amplitude of $\mathbb{B}\bar{\mathbb{B}} \to \bar{\mathbb{B}}\mathbb{B}$. Using crossing symmetry relations for systems with spin [43,74,75],[11] the amplitude for the t-channel process of $\mathbb{B}\mathbb{B} \to \mathbb{B}\mathbb{B}$ via the correlated $\pi\pi$ intermediate state with $IJ = 00$ can be expressed as

$$\begin{aligned}&\mathcal{M}^{t\text{-channel}}_{\mathbb{B}(\lambda_1)\mathbb{B}(\lambda_3)\to\mathbb{B}(\lambda_2)\mathbb{B}(\lambda_4),0}(t,s)\\&\quad=\sum_{\lambda_i'} d^{\frac{1}{2}}_{\lambda_1\lambda_1'}(\alpha_1)d^{\frac{1}{2}}_{\lambda_2\lambda_2'}(\alpha_2)d^{\frac{1}{2}}_{\lambda_3\lambda_3'}(\alpha_3)d^{\frac{1}{2}}_{\lambda_4\lambda_4'}(\alpha_4)\\&\qquad\times\mathcal{M}^{s\text{-channel}}_{\mathbb{B}(\lambda_1')\bar{\mathbb{B}}(\lambda_2')\to\bar{\mathbb{B}}(\lambda_3')\mathbb{B}(\lambda_4'),0}(s),\end{aligned}\tag{C1}$$

where α_i represents the Wigner rotation angles corresponding to the Lorentz transformation from the s-channel c.m. frame to the t-channel c.m. frame, and the subscript 0 signifies that the $\pi\pi$ of either the t-channel process or the s-channel process forms an isoscalar S-wave. Considering that the crossing relation, Eq. (C1), is solely dependent on the particles of the external lines, the same relation is applicable regardless of whether there is a σ exchange or a correlated $\pi\pi$ exchange, namely,

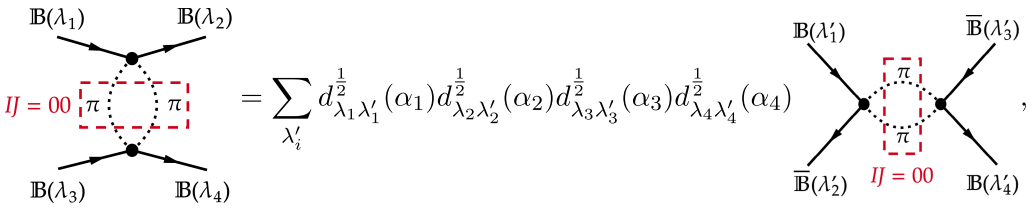

(C2)

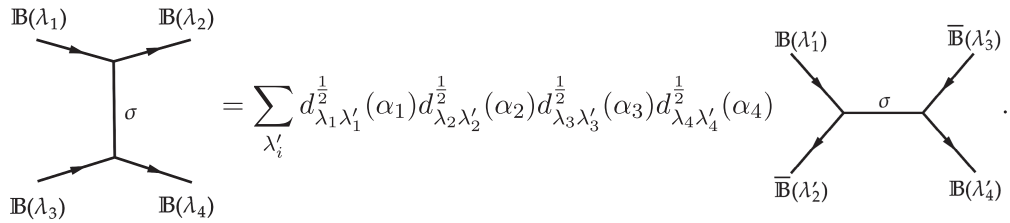

(C3)

We then obtain

[11] In the context of crossing relation, for a t-channel process of $\mathbb{B}(p_1) + \mathbb{B}(p_2) \to \mathbb{B}(p_3) + \mathbb{B}(p_4)$, as illustrated in Fig. 6, s refers to $(p_1 - p_3)^2$ while t refers to $(p_1 + p_2)^2$.

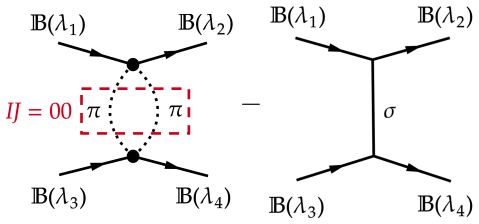

$$= \sum_{\lambda_i'} d^{\frac{1}{2}}_{\lambda_1\lambda_1'}(\alpha_1) d^{\frac{1}{2}}_{\lambda_2\lambda_2'}(\alpha_2) d^{\frac{1}{2}}_{\lambda_3\lambda_3'}(\alpha_3) d^{\frac{1}{2}}_{\lambda_4\lambda_4'}(\alpha_4)$$

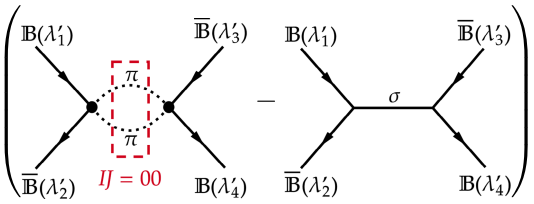

(C4)

Since our goal is to ensure that the amplitude of the correlated $\pi\pi$ exchange with $IJ = 00$ and that of the σ exchange are approximately the same for the t-channel process of $\mathbb{B}\mathbb{B} \to \mathbb{B}\mathbb{B}$ within the t-channel physical region, i.e., $t \geq 4m_{\mathbb{B}}^2$, we require the corresponding s-channel amplitudes of $\mathbb{B}\bar{\mathbb{B}} \to \bar{\mathbb{B}}\mathbb{B}$ to approximate each other as well as possible, i.e.,

$$\mathcal{M}^{\mathrm{OBE}}_{\mathbb{B}\bar{\mathbb{B}}\to\bar{\mathbb{B}}\mathbb{B}}(s) \simeq \mathcal{M}^{\mathrm{DR}}_{\mathbb{B}\bar{\mathbb{B}}\to\bar{\mathbb{B}}\mathbb{B},0}(s), \tag{C5}$$

when $s \in [4m_{\mathbb{B}}^2 - t, 0]$. The u-channel process mirrors this exactly.

[1] A. Hosaka, T. Iijima, K. Miyabayashi, Y. Sakai, and S. Yasui, Exotic hadrons with heavy flavors: X, Y, Z, and related states, Prog. Theor. Exp. Phys. **2016**, 062C01 (2016).

[2] J.-M. Richard, Exotic hadrons: Review and perspectives, Few-Body Syst. **57**, 1185 (2016).

[3] R. F. Lebed, R. E. Mitchell, and E. S. Swanson, Heavy-quark QCD exotica, Prog. Part. Nucl. Phys. **93**, 143 (2017).

[4] A. Esposito, A. Pilloni, and A. D. Polosa, Multiquark resonances, Phys. Rep. **668**, 1 (2017).

[5] A. Ali, J. S. Lange, and S. Stone, Exotics: Heavy pentaquarks and tetraquarks, Prog. Part. Nucl. Phys. **97**, 123 (2017).

[6] S. L. Olsen, T. Skwarnicki, and D. Zieminska, Nonstandard heavy mesons and baryons: Experimental evidence, Rev. Mod. Phys. **90**, 015003 (2018).

[7] F.-K. Guo, C. Hanhart, U.-G. Meißner, Q. Wang, Q. Zhao, and B.-S. Zou, Hadronic molecules, Rev. Mod. Phys. **90**, 015004 (2018); **94**, 029901(E) (2022).

[8] N. Brambilla, S. Eidelman, C. Hanhart, A. Nefediev, C.-P. Shen, C. E. Thomas, A. Vairo, and C.-Z. Yuan, The XYZ states: Experimental and theoretical status and perspectives, Phys. Rep. **873**, 1 (2020).

[9] Y. Yamaguchi, A. Hosaka, S. Takeuchi, and M. Takizawa, Heavy hadronic molecules with pion exchange and quark core couplings: A guide for practitioners, J. Phys. G **47**, 053001 (2020).

[10] X.-K. Dong, F.-K. Guo, and B.-S. Zou, A survey of heavy-antiheavy hadronic molecules, Prog. Phys. **41**, 65 (2021).

[11] X.-K. Dong, F.-K. Guo, and B.-S. Zou, A survey of heavy–heavy hadronic molecules, Commun. Theor. Phys. **73**, 125201 (2021).

[12] H.-X. Chen, W. Chen, X. Liu, Y.-R. Liu, and S.-L. Zhu, An updated review of the new hadron states, Rep. Prog. Phys. **86**, 026201 (2023).

[13] L. Meng, B. Wang, G.-J. Wang, and S.-L. Zhu, Chiral perturbation theory for heavy hadrons and chiral effective field theory for heavy hadronic molecules, Phys. Rep. **1019**, 1 (2023).

[14] M. Mai, U.-G. Meißner, and C. Urbach, Towards a theory of hadron resonances, Phys. Rep. **1001**, 1 (2023).

[15] X.-K. Dong, F.-K. Guo, and B.-S. Zou, Explaining the many threshold structures in the heavy-quark hadron spectrum, Phys. Rev. Lett. **126**, 152001 (2021).

[16] H. Yukawa, On the interaction of elementary particles I, Proc. Phys. Math. Soc. Jpn. **17**, 48 (1935).

[17] J. W. Durso, M. Saarela, G. E. Brown, and A. D. Jackson, Isobars, transition potentials and short range repulsion in the nucleon-nucleon interaction, Nucl. Phys. **A278**, 445 (1977).

[18] R. Machleidt, K. Holinde, and C. Elster, The Bonn meson exchange model for the nucleon nucleon interaction, Phys. Rep. **149**, 1 (1987).

[19] N. A. Törnqvist, From the deuteron to deusons, an analysis of deuteron-like meson meson bound states, Z. Phys. C **61**, 525 (1994).

[20] G.-J. Ding, J.-F. Liu, and M.-L. Yan, Dynamics of hadronic molecule in one-boson exchange approach and possible heavy flavor molecules, Phys. Rev. D **79**, 054005 (2009).

[21] A. Calle Cordon and E. Ruiz Arriola, Renormalization vs strong form factors for one boson exchange potentials, Phys. Rev. C **81**, 044002 (2010).

[22] Z.-F. Sun, J. He, X. Liu, Z.-G. Luo, and S.-L. Zhu, $Z_b(10610)^{\pm}$ and $Z_b(10650)^{\pm}$ as the $B^*\bar{B}$ and $B^*\bar{B}^*$ molecular states, Phys. Rev. D **84**, 054002 (2011).

[23] L. Zhao, N. Li, S.-L. Zhu, and B.-S. Zou, Meson-exchange model for the $\Lambda\bar{\Lambda}$ interaction, Phys. Rev. D **87**, 054034 (2013).

[24] M.-Z. Liu, T.-W. Wu, J.-J. Xie, M. Pavon Valderrama, and L.-S. Geng, $D\Xi$ and $D^*\Xi$ molecular states from one boson exchange, Phys. Rev. D **98**, 014014 (2018).

[25] M.-Z. Liu, T.-W. Wu, M. Pavon Valderrama, J.-J. Xie, and L.-S. Geng, Heavy-quark spin and flavor symmetry partners of the X(3872) revisited: What can we learn from the one boson exchange model?, Phys. Rev. D **99**, 094018 (2019).

[26] Z. Y. Zhou, G. Y. Qin, P. Zhang, Z. Xiao, H. Q. Zheng, and N. Wu, The pole structure of the unitary, crossing symmetric low energy $\pi\pi$ scattering amplitudes, J. High Energy Phys. 02 (2005) 043.

[27] I. Caprini, G. Colangelo, and H. Leutwyler, Mass and width of the lowest resonance in QCD, Phys. Rev. Lett. **96**, 132001 (2006).

[28] R. García-Martín, R. Kamiński, J. R. Peláez, and J. Ruiz de Elvira, Precise determination of the $f_0(600)$ and $f_0(980)$ pole parameters from a dispersive data analysis, Phys. Rev. Lett. **107**, 072001 (2011).

[29] J. R. Peláez, From controversy to precision on the sigma meson: A review on the status of the non-ordinary $f_0(500)$ resonance, Phys. Rep. **658**, 1 (2016).

[30] D.-L. Yao, L.-Y. Dai, H.-Q. Zheng, and Z.-Y. Zhou, A review on partial-wave dynamics with chiral effective field theory and dispersion relation, Rep. Prog. Phys. **84**, 076201 (2021).

[31] X.-H. Cao, Q.-Z. Li, Z.-H. Guo, and H.-Q. Zheng, Roy equation analyses of $\pi\pi$ scatterings at unphysical pion masses, Phys. Rev. D **108**, 034009 (2023).

[32] A. Rodas, J. J. Dudek, and R. G. Edwards, Constraining the quark mass dependence of the lightest resonance in QCD, arXiv:2304.03762.

[33] J. W. Durso, A. D. Jackson, and B. J. Verwest, Models of pseudophysical $N\bar{N} \to \pi\pi$ amplitudes, Nucl. Phys. **A345**, 471 (1980).

[34] B. Holzenkamp, K. Holinde, and J. Speth, A meson exchange model for the hyperon nucleon interaction, Nucl. Phys. **A500**, 485 (1989).

[35] U.-G. Meißner, Chiral dynamics: Where are the scalars?, Comments Nucl. Part. Phys. **20**, 119 (1991).

[36] D. Rönchen, M. Döring, F. Huang, H. Haberzettl, J. Haidenbauer, C. Hanhart, S. Krewald, U.-G. Meißner, and K. Nakayama, Coupled-channel dynamics in the reactions $\pi N \to \pi N, \eta N, K\Lambda, K\Sigma$, Eur. Phys. J. A **49**, 44 (2013).

[37] A. Reuber, K. Holinde, H.-C. Kim, and J. Speth, Correlated $\pi\pi$ and $K\bar{K}$ exchange in the baryon baryon interaction, Nucl. Phys. **A608**, 243 (1996).

[38] J. Haidenbauer and U.-G. Meißner, The Julich hyperon-nucleon model revisited, Phys. Rev. C **72**, 044005 (2005).

[39] J. F. Donoghue, Sigma exchange in the nuclear force and effective field theory, Phys. Lett. B **643**, 165 (2006).

[40] H.-J. Kim and H.-C. Kim, σ and ρ coupling constants for the charmed and beauty mesons, Phys. Rev. D **102**, 014026 (2020).

[41] N. Yalikun and B.-S. Zou, Anticharmed strange pentaquarks from the one-boson-exchange model, Phys. Rev. D **105**, 094026 (2022).

[42] J. Gasser and U.-G. Meißner, Chiral expansion of pion form factors beyond one loop, Nucl. Phys. **B357**, 90 (1991).

[43] A. D. Martin and T. D. Spearman, *Elementary Particle Theory* (North-Holland Publishing Co., Amsterdam, 1970).

[44] A. Krause, Baryon matrix elements of the vector current in chiral perturbation theory, Helv. Phys. Acta **63**, 3 (1990).

[45] M. Frink and U.-G. Meißner, Chiral extrapolations of baryon masses for unquenched three flavor lattice simulations, J. High Energy Phys. 07 (2004) 028.

[46] J. A. Oller, M. Verbeni, and J. Prades, Meson-baryon effective chiral Lagrangians to $O(q^3)$, J. High Energy Phys. 09 (2006) 079.

[47] M. Mai and U.-G. Meißner, New insights into antikaon-nucleon scattering and the structure of the $\Lambda(1405)$, Nucl. Phys. **A900**, 51 (2013).

[48] X.-L. Ren, L. S. Geng, J. Martin Camalich, J. Meng, and H. Toki, Octet baryon masses in next-to-next-to-next-to-leading order covariant baryon chiral perturbation theory, J. High Energy Phys. 12 (**2012**) 073.

[49] M. Jacob and G. C. Wick, On the general theory of collisions for particles with spin, Ann. Phys. (N.Y.) **7**, 404 (1959).

[50] G. Amoros, J. Bijnens, and P. Talavera, QCD isospin breaking in meson masses, decay constants and quark mass ratios, Nucl. Phys. **B602**, 87 (2001).

[51] R. Omnès, On the solution of certain singular integral equations of quantum field theory, Nuovo Cimento **8**, 316 (1958).

[52] R. García-Martín, R. Kamiński, J. R. Peláez, J. Ruiz de Elvira, and F. J. Ynduráin, The pion-pion scattering amplitude. IV: Improved analysis with once subtracted Roy-like equations up to 1100 MeV, Phys. Rev. D **83**, 074004 (2011).

[53] S. Ropertz, C. Hanhart, and B. Kubis, A new parametrization for the scalar pion form factors, Eur. Phys. J. C **78**, 1000 (2018).

[54] J. F. Donoghue, Dispersion relations and effective field theory, in *Advanced School on Effective Theories* (1996), arXiv:hep-ph/9607351.

[55] X.-W. Kang, B. Kubis, C. Hanhart, and U.-G. Meißner, B_{l4} decays and the extraction of $|V_{ub}|$, Phys. Rev. D **89**, 053015 (2014).

[56] Y.-H. Chen, J. T. Daub, F.-K. Guo, B. Kubis, U.-G. Meißner, and B.-S. Zou, Effect of Z_b states on $\Upsilon(3S) \to \Upsilon(1S)\pi\pi$ decays, Phys. Rev. D **93**, 034030 (2016).

[57] X.-K. Dong, V. Baru, F.-K. Guo, C. Hanhart, A. Nefediev, and B.-S. Zou, Is the existence of a $J/\psi J/\psi$ bound state plausible?, Sci. Bull. **66**, 2462 (2021).

[58] Y.-H. Chen, Chromopolarizability of charmonium and $\pi\pi$ final state interaction revisited, Adv. High Energy Phys. **2019**, 7650678 (2019).

[59] A. V. Anisovich and H. Leutwyler, Dispersive analysis of the decay $\eta \to 3\pi$, Phys. Lett. B **375**, 335 (1996).

[60] G. Colangelo, S. Lanz, H. Leutwyler, and E. Passemar, Dispersive analysis of $\eta \to 3\pi$, Eur. Phys. J. C **78**, 947 (2018).
[61] M. Gell-Mann and M. Lévy, The axial vector current in beta decay, Nuovo Cimento **16**, 705 (1960).
[62] E. Oset, H. Toki, M. Mizobe, and T. T. Takahashi, sigma exchange in the NN interaction within the chiral unitary approach, Prog. Theor. Phys. **103**, 351 (2000).
[63] M. Hoferichter, J. Ruiz de Elvira, B. Kubis, and U.-G. Meißner, Roy–Steiner-equation analysis of pion–nucleon scattering, Phys. Rep. **625**, 1 (2016).
[64] M. Hoferichter, J. Ruiz de Elvira, B. Kubis, and U.-G. Meißner, Matching pion-nucleon Roy-Steiner equations to chiral perturbation theory, Phys. Rev. Lett. **115**, 192301 (2015).
[65] J. J. de Swart, The octet model and its Clebsch-Gordan coefficients, Rev. Mod. Phys. **35**, 916 (1963); **37**, 326(E) (1965).
[66] N. Fettes, U.-G. Meißner, and S. Steininger, Pion-nucleon scattering in chiral perturbation theory. 1. Isospin symmetric case, Nucl. Phys. **A640**, 199 (1998).
[67] N. Fettes, U.-G. Meißner, M. Mojžiš, and S. Steininger, The chiral effective pion-nucleon Lagrangian of order p^{4*}, Ann. Phys. (N.Y.) **283**, 273 (2000); **288**, 249(E) (2001).
[68] S. Scherer and M. R. Schindler, *A Primer for Chiral Perturbation Theory*, Springer Lecture Notes in Physics Vol. 830 (Springer, Heidelberg, 2012).
[69] U.-G. Meißner and A. Rusetsky, *Effective Field Theories* (Cambridge University Press, Cambridge, England, 2022).
[70] M. Hoferichter, J. R. de Elvira, B. Kubis, and U.-G. Meißner, Nucleon resonance parameters from Roy-Steiner equations, arXiv:2312.15015.
[71] B. Borasoy and U.-G. Meißner, Chiral expansion of baryon masses and σ-terms, Ann. Phys. (Amsterdam) **254**, 192 (1997).
[72] Y. Ikeda, T. Hyodo, and W. Weise, Chiral SU(3) theory of antikaon-nucleon interactions with improved threshold constraints, Nucl. Phys. **A881**, 98 (2012).
[73] Z.-H. Guo and J. A. Oller, Meson-baryon reactions with strangeness -1 within a chiral framework, Phys. Rev. C **87**, 035202 (2013).
[74] Y. Hara, On crossing relations for helicity amplitudes, J. Math. Phys. (N.Y.) **11**, 253 (1970).
[75] A. Hebbar, D. Karateev, and J. Penedones, Spinning S-matrix bootstrap in 4d, J. High Energy Phys. 01 (2022) 060.